Adaptive parametric model order reduction technique for optimization of vibro-acoustic models: Application to hearing aid design

Creixell Mediante, Ester; Jensen, Jakob Søndergaard; Naets, Frank; Brunskog, Jonas; Larsen, Martin

Published in:
Journal of Sound and Vibration

Link to article, DOI:
10.1016/j.jsv.2018.03.013

Publication date:
2018

Document Version
Peer reviewed version

Adaptive parametric model order reduction technique for optimization of vibro-acoustic models: Application to hearing aid design. ☆

Ester Creixell-Mediante[a,b,*], Jakob S. Jensen[a], Frank Naets[c,d], Jonas Brunskog[a], Martin Larsen[b]

[a] *Acoustic Technology, Department of Electrical Engineering, Technical University of Denmark, Ørsteds Plads 352, 2800 Kgs. Lyngby, Denmark*
[b] *Oticon A/S, Kongebakken 9, 9765 Smørum, Denmark*
[c] *Department of Mechanical Engineering, KU Leuven, Celestijnenlaan 300B, B-3001 Heverlee, Leuven, Belgium*
[d] *Fellow of Flanders Make*

Abstract

Finite Element (FE) models of complex structural-acoustic coupled systems can require a large number of degrees of freedom in order to capture their physical behaviour. This is the case in the hearing aid field, where acoustic-mechanical feedback paths are a key factor in the overall system performance and modelling them accurately requires a precise description of the strong interaction between the light-weight parts and the internal and surrounding air over a wide frequency range. Parametric optimization of the FE model can be used to reduce the vibroacoustic feedback in a device during the design phase; however, it requires solving the model iteratively for multiple frequencies at different parameter values, which becomes highly time consuming when the system is large. Parametric Model Order Reduction (pMOR) techniques aim at reducing the computational cost associated with each analysis by projecting the full system into a reduced space. A drawback of most of the existing techniques is that the vector basis of the reduced space is built at an offline phase where the full system must be solved for a large sample of parameter values, which can also become highly time consuming. In this work, we present an adaptive pMOR technique where the construction of the projection basis is embedded in the optimization process and requires fewer full system analyses, while the accuracy of the reduced system is monitored by a cheap error indicator. The performance of the proposed method is evaluated for a 4-parameter optimization of a frequency response for a hearing aid model, evaluated at 300 frequencies, where the objective function evaluations become more than one order of magnitude faster than for the full system.

Keywords: Model Reduction, Optimization, Structure-acoustic interaction

1. Introduction

Simulation is gaining relevance in industrial design procedures, which have evolved from a purely prototyping and testing approach to a context where numerical simulation is used from the early phases. Obtaining reliable models is a key point in the design process, and as more and more accuracy is required, the complexity of the models increases. In the field of hearing aids, numerical vibro-acoustic analysis is essential for the study of problems such as feedback; currently the main gain limiting factor of the hearing devices. The high number of small parts that conform them, the strong structure-acoustic interaction between those parts and the internal air volume require models with a large number of Degrees Of Freedom (DOFs) in order to capture the physical behavior accurately. Therefore, significant computational challenges are encountered

☆ Part of this work was presented in Internoise 2016 and ISMA 2016

* Corresponding author
Email addresses: emed@oticon.com (Ester Creixell-Mediante), json@elektro.dtu.dk (Jakob S. Jensen), frank.naets@kuleuven.be (Frank Naets), jbr@elektro.dtu.dk (Jonas Brunskog), mnla@oticon.com (Martin Larsen)

when solving problems that require iterative and/or repeated solutions of the numerical model. Tasks such as uncertainty analysis by means of Monte-Carlo methods, or parametric and topology optimization, require solving the system of model equations repeatedly for a large number of variations of different parameters. Therefore, the time required for solving the numerical problem at each iteration becomes a critical factor. In the present work, we develop an adaptive model order reduction technique and apply it to a hearing aid design problem.

In a recent paper [1], topology optimization of a part of a hearing instrument including structure-acoustic interaction was performed. Optimizing one part of the device requires the complete assembly to be taken into account when there is a strong acoustic-mechanical interaction, since the multiple vibrational and acoustic transmission paths between parts have a significant influence on the system performance. To facilitate the study, the performance was evaluated and optimized for a limited number of frequencies; therefore, the effects at the rest of the frequency range were not controlled. This highlights the need to develop computational reduction techniques that allow optimization to be carried out with a higher level of accuracy and frequency resolution.

Model order reduction techniques have been described in the literature and applied in several fields [2, 3, 4]. The earliest research on the topic deals with structural dynamics problems, with the Component Mode Synthesis (CMS) method being developed in the 1960s [5, 6]. When modal-based methods were to be extended to problems with structure-acoustic interaction, different approaches were developed to construct the reduction basis. Since solving the coupled eigenvalue problem requires higher computational effort due to the asymmetric nature of the matrices when the pressure-displacement formulation is used, one suggested approach [7] consisted in using the uncoupled structural and acoustic modes, which is an efficient solution for problems with a weak structure-acoustic coupling. However, for problems with strong interaction, a large amount of modes are required in order to obtain an accurate reduced model [8], making it a poorly efficient technique. With the recent improvements on eigenvalue solvers and computational power, solving the asymmetric problem has become less challenging; therefore, the coupled modal vectors, that better describe true behavior of the system, can now be used in practice. Another issue that arises from the asymmetry of the matrices is that the modal vectors do not form an orthogonal basis, which has been addressed in the literature in two ways: by using both left and right eigenvectors [9, 10], or by applying orthogonalization techniques on the right eigenvectors [11]. The two approaches have been compared by the authors in Ref. [12], which showed that the second approach is more suited to the present problem, and is therefore employed in this work.

In CMS, the model is divided in substructures, which are reduced internally while the interface DOFs are kept unmodified. Even though interface reduction methods have been developed [13, 14], this method is most efficient for systems that can be divided at low-dimensional interfaces, such as the pipes studied in Ref. [11], but it can be difficult to efficiently substructure systems that consist of complex 3D parts, as in hearing aid models. Despite the cost of solving the full eigenvalue problem, it turns out that a more efficient technique [15] consists in reducing the complete structure in terms of the global modal vectors, since fine resolution frequency response calculations can then be done at a very low computational cost on the reduced system. Therefore, this approach is selected in our work.

For parametric optimization purposes, a new modal reduction basis would have to be calculated for each variation of the parameter values when using the suggested approach (unless the modal vectors are not sensitive to the parameters, as assumed in Refs. [16, 17]). This would still be faster than calculating the full system frequency response if the number of considered frequencies is large; however, parametric Model Order Reduction (pMOR) techniques have been developed to make this process even more efficient. The Multi-Model Reduction (MMR) technique is one of the most straight-forward pMOR methods, which consists in constructing a global reduction basis that is valid for any value of the parameters within a given design domain by concatenating the modal vectors calculated at several points in the parameter space in a global reduction matrix [4, 18]. The number of included points should be sufficient to ensure that the reduc-

tion error at any point in the domain is below a required level. The resulting global vector matrix is then orthogonalized, since some modal vectors calculated at different sampled points can be linearly dependent, and they would otherwise result in ill-conditioning. When using MMR for coupled problems, the fact that the modal vectors resulting from the asymmetric matrix system are inherently not orthogonal should also be taken into account.

The MMR technique is usually applied in an offline-online fashion, where the reduction basis is constructed first (offline) and used for very fast function evaluation during the optimization (online). A drawback of this approach is that the offline phase can become very costly for an increasing number of parameters, since (a) the full model eigenvalue problem must be solved for each point that is included in the basis, and (b) the full model solution must be calculated at a representative sample of non-included points to evaluate the reduction error and ensure accuracy. To avoid problem (b), error bounds or error estimators that are cheaper to compute can be used instead of the true error [19]. Tight error bounds can be found for specific types of partial differential equations [20]; however, we will use a residual-based error indicator in this work, since they can be applied for any kind of problem and have already been successfully used in frequency response calculation problems [21].

A key point for reducing the computational time due to problem (a) is minimizing the number of points that need to be included in the basis. Greedy algorithms have been suggested for this purpose [22, 23, 24, 25]; they consist in iteratively finding the point of the domain where the reduction error is maximal and adding it to the basis, until the maximum error is below some requirement. These methods are most efficient for applications like uncertainty characterization studies or system control, where most of the parameter domain is evaluated in the online phase. However, for optimization problems, only a small part of this domain is actually explored, and the efforts made for accurately representing points that will not be evaluated during the optimization are unnecessary. To exploit this feature, an adaptive reduced order basis construction approach that breaks the offline-online framework is proposed in this work. Previous works in this direction can be found in Refs. [26, 27], where a method based on trust-region optimization is suggested; however, those approaches require solving a series of optimization problems bounded by an error estimator, which only results in an efficiency improvement when a very cheap error bound is available. Since we choose to use a residual-based error indicator, this approach does not lead to an efficient framework in the considered case. A more straight-forward basis updating methodology is therefore developed in this work. The suggested approach consists in updating the reduced order basis during the course of the optimization by evaluating the error indicator at each objective function calculation and adding the current point if it drops below a selected threshold. A similar approach is used in Ref. [28] for static structural topology optimization problems.

The main contributions by the authors are the extension of the MMR technique to vibroacoustic modal reduction bases, the development of a state vector error indicator adequate for such bases, and the algorithm for adaptively updating the reduced order basis during the optimization. This article is organized as follows. In section 2, the hearing aid study case model and optimization problem that will be used for testing the algorithm suggested in this paper are presented. In section 3, the details of the proposed adaptive pMOR optimization technique are described. In section 4, the performance of the method is evaluated for the proposed case, and section 5 summarizes the conclusions. All numerical tests were performed on a regular desktop computer (Intel Core i7-4790k, 4 GHz CPU and 32 GB of RAM memory).

2. Test case: hearing aid design optimization problem

A main objective during the design phase of a hearing aid is the minimization of feedback paths, i.e. the acoustic and vibratory isolation of the microphones (which capture the outer acoustic signal, but are also sensitive to vibration) from the receiver (the loudspeaker that emits the sound into the ear, which also introduces structural vibration) to avoid signal loops. Even though powerful Digital Signal Processing (DSP) feedback cancellation algorithms are implemented in most hearing instruments, a design that maximizes the

isolation between the transducers from a physical point of view is a key aspect for the final performance of the product. This motivates the use of FE models for frequency response optimization of the hearing aid. The models can however become very large, since the maximum frequency of interest goes up to 10 kHz, requiring a highly refined mesh especially for parts with soft materials and for the air volumes. Moreover, the frequency resolution of the optimized response should be fine enough to capture the complex behaviour of the system, requiring solutions for a high number of frequencies. These factors make the vibroacoustic response calculation highly time consuming and its optimization practically impossible, which triggers the need for the application of model order reduction techniques.

2.1. Problem statement

Hearing aids are formed by a large number of small parts connected to each other. One of the most critical components in the design is the receiver (loudspeaker) suspension, since its main role is the isolation of the receiver from the rest of the system. The tube that brings the sound from the receiver output to the ear is also a potential source of feedback, since it interacts strongly with the inner air due to its soft material and thin dimensions. In this study, we consider the optimization of the Young's modulus and thickness of these two parts to minimize the vibration velocity at the microphone position over the usual frequency range of interest in hearing aid design: between 100 Hz and 10kHz.

A simplified model of a Behind The Ear (BTE) hearing aid, shown in Figure 1, is built for this purpose. The parts that play a main role in the vibro-acoustic response are included, being the suspension, the tube and the receiver (simplified as a steel block), and the remaining components are modelled as a single solid body. The acoustic domain consists of a hard-walled acoustic volume, the coupler that simulates the acoustic impedance of the ear, an air canal that connects it to the receiver output through the tube and the suspension, and a small air cavity surrounding the receiver and the suspension. For the sake of simplicity and since the specific purpose of this study is evaluating the performance of the suggested model order reduction method, the air that surrounds the hearing aid and the transducer models of the receiver and the microphones are not included in the calculation. However, the acoustic and vibratory excitation signals are obtained from a lumped element model of the receiver, and applied as a frequency-dependent particle velocity and two directional forces, shown in Figure 2, at a point on the surface between the receiver and the air canal.

2.2. Model set-up and optimization problem

The model has been set up in ANSYS® Academic Research Release 17.1, and the ANSYS® acoustic extension v171.4. Even though the maximum frequency of interest is 10 kHz, modal extraction will be performed with the model up to 12 kHz for model reduction purposes, as will be explained in the next section; therefore, the size of the mesh of the complete model has been determined by a convergence study of the eigenfrequencies of the system up to 12 kHz, resulting in 90821 DOFs, where the suspension requires the finest mesh in order to capture its rich modal behaviour. The nominal material properties for each part can be seen in Table 1.

	Density (ρ) [kg/m^3]	Young's modulus (E) [Pa]	Poisson ratio (σ)	Damping coefficient (ν)[%]
Body	1040	$2 \cdot 10^9$	0.4	0
Tube	1300	$1 \cdot 10^8$	0.4	0.2
Receiver	7850	$2 \cdot 10^{11}$	0.3	0
Suspension	1100	$6 \cdot 10^6$	0.49	0.1

Table 1: Nominal material properties of the hearing aid

In hearing aids, thermo-viscous losses become important in thin tubes and small cavities. They are usually modelled by a Boundary Layer Impedance (BLI) model [29], implemented in the ANSYS® FLUID

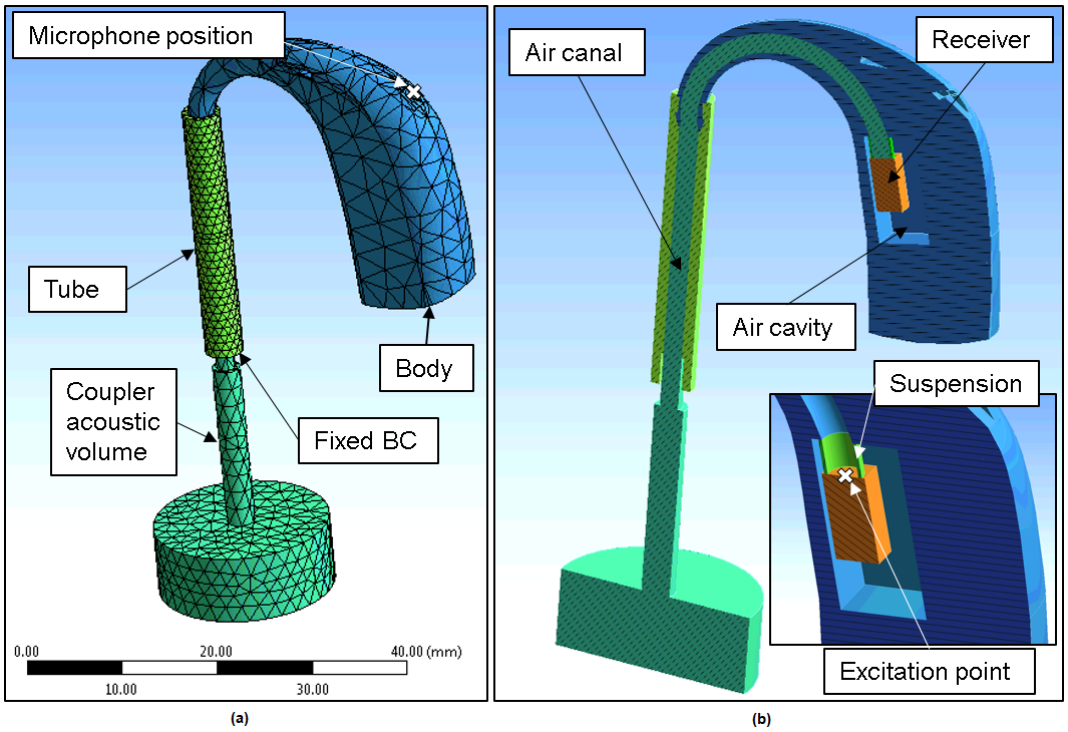

Figure 1: Considered hearing aid model. (a) View of the model from outside, without outer air. (b) View of the vertically sliced model with zoomed view of the suspension and its surrounding area.

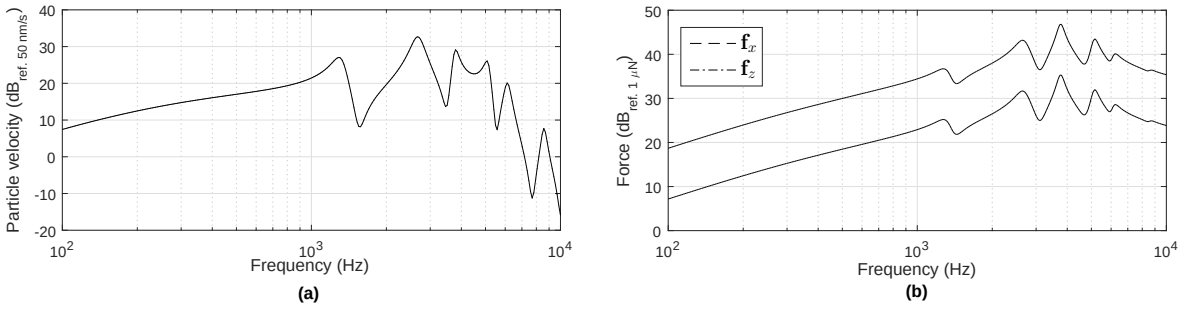

Figure 2: Particle velocity (a) and forces (b) obtained from the receiver lumped element model.

elements (FLUID220 and FLUID221 are used in the model), which is frequency-dependent. Since losses in the air canal have an effect on the velocity response at the microphone position in the presented model, as shown by the solid and dashed lines in Figure 3, it is important to include them to avoid optimizing a non-realistic peaky curve. However, reducing a system with frequency-dependent properties is significantly more cumbersome than a frequency-independent one. Therefore, a simplified version of the loss model is applied here, where the BLI effect is only calculated at 1000 Hz and added as a constant matrix to the system along the full frequency range. The resulting response is shown by the dotted line in Figure 3, which is almost on top of the solid line. Even though the response is not exactly the same, we hypothesize that using this approximation during the optimization will lead in practice to a result that is also close to optimal when the full BLI model is applied. This hypothesis will be validated in Section 4, where the results are presented.

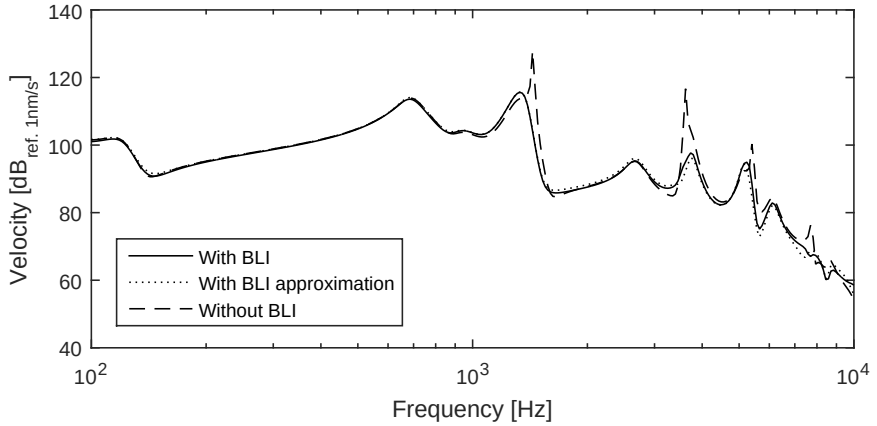

Figure 3: Comparison of the total velocity at the microphone position when applying BLI, the frequency-independent BLI approximation, and no losses

When the pressure-displacement formulation is used, the equation of motion in the frequency domain of the complete system under harmonic excitation takes the form

$$\left(\begin{bmatrix} \mathbf{K}_s & -\mathbf{S}^T \\ \mathbf{0} & \mathbf{K}_a \end{bmatrix} - \omega^2 \begin{bmatrix} \mathbf{M}_s & \mathbf{0} \\ \rho_a \mathbf{S} & \mathbf{M}_a \end{bmatrix} \right) \begin{Bmatrix} \mathbf{x}_s \\ \mathbf{p}_a \end{Bmatrix} = \begin{Bmatrix} \mathbf{f}_s \\ \mathbf{f}_a \end{Bmatrix}, \tag{1}$$

where $\mathbf{K}_s$ and $\mathbf{M}_s$ are the structural stiffness and mass matrices, $\mathbf{K}_a$ and $\mathbf{M}_a$ are the acoustic stiffness and mass matrices, $\mathbf{S}$ is the fluid-structure interaction coupling matrix, ρ_a is the density of the acoustic medium, ω is the frequency, $\mathbf{x}_s$ is the vector of structural displacements, $\mathbf{p}_a$ is the vector of acoustic pressures, $\mathbf{f}_s$ is the vector of external structural forces and $\mathbf{f}_a$ is the vector of external acoustic excitations. In this model, the damping matrix vanishes since only hysteretic material damping is considered, which is included as the imaginary part to the structural stiffness matrix, $\mathbf{K}_s$, and the terms associated with the BLI are included as a constant matrix added to the stiffness matrix, $\mathbf{K}_a$.

The optimization problem we consider in this work can be formulated as

$$\begin{aligned} &\underset{\boldsymbol{\mu}}{\text{minimize}} \; g(\boldsymbol{\mu}) = 10 \log \sum_{k=1}^{K} \left| \frac{\mathbf{v}_m(\boldsymbol{\mu}, k)}{v_{ref}} \right|^2 \\ &\text{subject to} \qquad\qquad \boldsymbol{\mu}_l \geq \boldsymbol{\mu} \geq \boldsymbol{\mu}_u, \end{aligned} \tag{2}$$

where $|\mathbf{v}_m(\boldsymbol{\mu}, k)|$ is the magnitude of the total velocity at a node on the microphone position, calculated as $\left| \sqrt{v_{mx}^2 + v_{my}^2 + v_{mz}^2} \right|$, v_{ref} is the reference structural velocity, k is the k-th discrete frequency line and K is

the total number of frequencies (300 frequencies logarithmically distributed between 100 Hz and 10 kHz in this case). The vector $\boldsymbol{\mu}$ contains the four considered optimization parameters: the Young's moduli and the thicknesses of the tube and the suspension:

$$\boldsymbol{\mu} = \begin{bmatrix} E_t \\ E_s \\ t_t \\ t_s \end{bmatrix}, \tag{3}$$

which can vary within the lower and upper bounds, $\boldsymbol{\mu}_l$ and $\boldsymbol{\mu}_u$, specified in Table 2.

	Lower bound $\boldsymbol{\mu}_l$	Upper bound $\boldsymbol{\mu}_u$	Initial value $\boldsymbol{\mu}_0$
Tube E modulus [Pa]	$9 \cdot 10^7$	10^9	10^8
Tube thickness [mm]	0.96	1.4	1
Suspension E modulus [Pa]	10^6	10^8	$6 \cdot 10^6$
Suspension thickness [mm]	0.175	0.225	0.2

Table 2: Parameter design space

The thickness modification is done by moving all the nodes on the outer surface of the tube or the suspension, respectively, in the direction normal to the surface. The upper and lower bounds are therefore determined by the amount of deformation that can be applied before the mesh becomes too distorted.

2.3. Optimization framework with full model

The optimization is performed in MATLAB® , using a constrained optimization algorithm implemented in the MATLAB® Optimization Toolbox [30] function *fmincon* (a detailed description of this method can be found in ref. [31]) and the gradient is calculated using finite differences. Therefore, at each optimization iteration, the objective function in Eq. 2 must be evaluated at least 5 times: for the current point and for the calculation of each component of the gradient. For each function evaluation, MATLAB® interfaces with ANSYS® to update the design parameters and command building the new system matrices, which are then read into MATLAB® , where the system in Eq. 1 is reduced and solved for the different frequency lines, as will be explained in the following sections, and the objective function value is calculated. The algorithm stops the optimization when the size of the step or the variation of the objective function between two consecutive iterations is below a specified tolerance.

If the full system in Eq. 1 is solved without reduction, the computational time required for a single objective function evaluation is around 2.4 hours, which is spent in different steps as detailed in Table 3. Even though a significant amount of time is spent in the communication between softwares, the largest burden is clearly on the response calculation, which is proportional to the number of considered frequencies. The proposed model order reduction technique focuses on reducing the time spent at that step.

	Building matrices in ANSYS® and importing into MATLAB®	Solving eq. 1 @ 300 freq. lines	Total
Time [s]	255	8500	8755 (2.4 hours)

Table 3: Objective function evaluation computational times for the full system

3. Adaptive model order reduction method for parametric optimization

In this chapter, the proposed framework for optimization using reduced order modeling is described. A model order reduction technique for vibroacoustic problems is developed in section 3.1, and the procedure to make it adaptive for parametric optimization problems is described in section 3.2.

3.1. Modal-based reduction for structural-acoustic coupling problems

A projection-based approach to Model Order Reduction (MOR) [4] is adopted in this work. In this approach the state vector $\mathbf{x} \in \mathbb{R}^n$ is approximated by a lower rank basis $\mathbf{T} \in \mathbb{R}^{\mathbf{n}\times\mathbf{m}}$:

$$\mathbf{x} \approx \mathbf{T}\mathbf{x}_r, \tag{4}$$

where $\mathbf{x}_r \in \mathbb{R}^m$ is the reduced state vector, and $m < n$.

In this work we employ a Galerkin projection such that for a generalized dynamic stiffness matrix and external load, the reduced equations of motion in the frequency domain can be written as:

$$\mathbf{T}^T\mathbf{D}\mathbf{T}\mathbf{x}_r = \mathbf{T}^T\mathbf{f}, \tag{5}$$

or

$$\mathbf{D}_r\mathbf{x}_r = \mathbf{f}_r, \tag{6}$$

where $\mathbf{D}_r \in \mathbb{R}^{m\times m}$ is the reduced generalized dynamic stiffness matrix. The construction of matrix $\mathbf{T}$ is discussed in the following.

Modal vectors have been widely used in model reduction of structural problems, since they form an orthogonal set which is easy to truncate according to their modal frequency and the maximum frequency of interest in the analysis. They are good descriptors of the system dynamics and have a clear physical interpretation, which have made them a popular choice also in the field of vibro-acoustics. In this section, the challenges encountered to obtain an efficient and accurate modal basis for vibro-acoustic problems, and more specifically for the hearing aid problem introduced in Section 2, are discussed.

The coupled eigenvalue problem must be solved to obtain the modal vectors. For the problem stated in eq. (1), it takes the following form:

$$\left(\underbrace{\begin{bmatrix} \mathbf{K}_s & -\mathbf{S}^T \\ \mathbf{0} & \mathbf{K}_a \end{bmatrix}}_{\mathbf{K}} - \lambda_i^2 \underbrace{\begin{bmatrix} \mathbf{M}_s & \mathbf{0} \\ \rho_a\mathbf{S} & \mathbf{M}_a \end{bmatrix}}_{\mathbf{M}} \right) \begin{Bmatrix} \boldsymbol{\psi}_s^i \\ \boldsymbol{\psi}_a^i \end{Bmatrix} = \begin{Bmatrix} \mathbf{0} \\ \mathbf{0} \end{Bmatrix}, \tag{7}$$

where $\{\boldsymbol{\psi}_s^i\}$ is the structural displacement part of the i-th modal vector, $\{\boldsymbol{\psi}_a^i\}$ is the acoustic pressure part of the i-th modal vector, and λ_i is the i-th eigenvalue given by $\lambda_i = \omega_i + j\delta_i$, δ_i/ω_i being the modal damping ratio, and ω_i the damped modal angular frequency. Note that these modal vectors are representing the full coupled system, and are not the uncoupled modal vectors as used in [7]. Since only those modes with a frequency below a required threshold, ω_t, are needed for the reduction, the truncated structural and acoustic modal matrices, $\boldsymbol{\Psi}_s = [\boldsymbol{\psi}_s^1, ..., \boldsymbol{\psi}_s^N]$ and $\boldsymbol{\Psi}_a = [\boldsymbol{\psi}_a^1, ..., \boldsymbol{\psi}_a^N]$ with $\omega_N < \omega_t$, can be obtained most efficiently by solving the eigenvalue problem with an iterative algorithm that stops after obtaining all modes below the selected frequency, such as the "Unsymmetric Method" used by the ANSYS® software [32].

Unlike for the purely structural case, the system matrices $\mathbf{M}$ and $\mathbf{K}$ are unsymmetric due to the coupling terms. This results in the right eigenvectors not being mutually orthogonal, which makes them not directly suitable as a reduced order basis. Based on the results of previous investigations by the authors [12], the

proposed approach consists in separating the acoustic and structural fields from the coupled modal vectors and orthogonalizing them with respect to the acoustic and structural mass matrices respectively, so that

$$\hat{\mathbf{\Psi}}_a^T \mathbf{M}_a \hat{\mathbf{\Psi}}_a = \mathbf{I} \tag{8}$$

$$\hat{\mathbf{\Psi}}_s^T \mathbf{M}_s \hat{\mathbf{\Psi}}_s = \mathbf{I}, \tag{9}$$

where $\hat{(\cdot)}$ indicates that the matrix has been orthogonalized. The orthogonalization procedure is detailed in the following for matrix $\hat{\mathbf{\Psi}}_a$, and is valid for all matrix orthogonalizations indicated in this paper with $\hat{(\cdot)}$.

Due to splitting the modal vectors into their acoustic and structural fields, the partial modal matrices $\mathbf{\Psi}_a$ and $\mathbf{\Psi}_s$ can contain linearly dependent vectors, which must be removed from the basis to avoid ill-conditioning. The vector products linked to the kinetic and strain energy are a good measure of independence [18], therefore we choose to construct a basis that is mass orthonormal here. This is done by performing a Singular Value Decomposition (SVD) of the mass-weighted vector product,

$$\mathbf{\Psi}_a^T \mathbf{M}_a \mathbf{\Psi}_a = \mathbf{U} \mathbf{\Sigma} \mathbf{V}^T, \tag{10}$$

where $\mathbf{\Sigma}$ is a diagonal matrix with the singular values on its diagonal and $\mathbf{U}$ and $\mathbf{V}$ are unitary matrices, which are also equal and orthogonal since the decomposed matrix is symmetric, and therefore $(\mathbf{V}^{-1})^T = \mathbf{V} = \mathbf{U}$. For eliminating the linearly dependent basis vectors, the columns of matrix $\mathbf{U}$ for which the singular value is below a certain threshold are discarded, yielding the truncated matrix $\mathbf{U}_t$. Theoretically, this threshold would be zero; however, due to the numerical noise involved in real computations, a recommended value for the threshold is a multiple of the floating-point relative accuracy [33], weighted by the largest singular value and the number of vectors in $\mathbf{\Psi}_a$ (in order to penalize large reduced models [18]). Substituting $\mathbf{U}$ by $\mathbf{U}_t$ in eq. (10), moving the right-hand side terms to the left side and equating it to eq. (8), we obtain

$$\hat{\mathbf{\Psi}}_a = \mathbf{\Psi}_a \mathbf{U}_t \mathbf{\Sigma}^{-1/2}. \tag{11}$$

The resulting orthogonalized modal matrices are then grouped to form the reduction basis as

$$\mathbf{T} = \begin{bmatrix} \hat{\mathbf{\Psi}}_s & \mathbf{0} \\ \mathbf{0} & \hat{\mathbf{\Psi}}_a \end{bmatrix}. \tag{12}$$

For the hearing aid model described in section 2 with the nominal parameter values, calculating the eigenmodes up to 12 kHz in ANSYS® takes 160 s and yields a reduction basis with 94 vectors. The error introduced by the reduction can be quantified by comparing the solution of the full system to the reconstructed solution of the reduced system. In terms of the 2-norm, the relative reduction error on the state response vector as a function of frequency is

$$\epsilon(\omega) = \frac{||\mathbf{x}(\omega) - \tilde{\mathbf{x}}(\omega)||_2}{||\mathbf{x}(\omega)||_2}, \tag{13}$$

which is shown by the grey line ("no enrichment") in Figure 4 for the reduction with modes below 12 kHz. The 1% error line is also shown, since it is commonly used as a pragmatic maximum reduction error level allowed to ensure accuracy. The relative error is above this line for frequencies above 2 kHz; therefore, the current reduction basis is not accurate enough for the system under study.

An efficient way to improve the accuracy of the reduced order model consists in enriching the reduction basis by including information about the external excitation [34]. The basis can be enriched with a static response, or with several dynamic responses calculated at selected frequencies. For a given frequency ω_k, an enrichment vector $\mathbf{x}_k$ is obtained by solving the full model at that frequency,

$$\mathbf{x}_k = \left(\mathbf{K} - \omega_k^2 \mathbf{M}\right)^{-1} \mathbf{f}(\omega_k). \tag{14}$$

The obtained set of enrichment vectors is not necessarily orthogonal; therefore, the same procedure as for the modal vectors is applied. The acoustic and structural parts of the response vectors are grouped separately in $\mathbf{X}_a$ and $\mathbf{X}_s$, which are orthogonalized following the technique described above to obtain $\hat{\mathbf{X}}_a$ and $\hat{\mathbf{X}}_s$. Then, the final reduced order basis is formed by concatenating them with the orthogonalized modal matrices, as

$$\mathbf{T} = \begin{bmatrix} \begin{bmatrix} \hat{\boldsymbol{\Psi}}_s \ \hat{\mathbf{X}}_s \end{bmatrix} & \mathbf{0} \\ \mathbf{0} & \begin{bmatrix} \hat{\boldsymbol{\Psi}}_a \ \hat{\mathbf{X}}_a \end{bmatrix} \end{bmatrix}. \tag{15}$$

When enriching the previously calculated modal basis with dynamic responses, we find that 4 enrichment vectors calculated at 100 Hz, 1 kHz, 7 kHz and 10 kHz are needed for the error to be below the desired level, as shown in Figure 4. This yields a reduced order basis with 102 basis vectors, only 8 more than for the original modal basis, consisting of 94. The time required for solving this reduced system at 300 frequencies is 9 s, which is 945 times shorter than the full system solution time, which took 8500 s (Table 3).

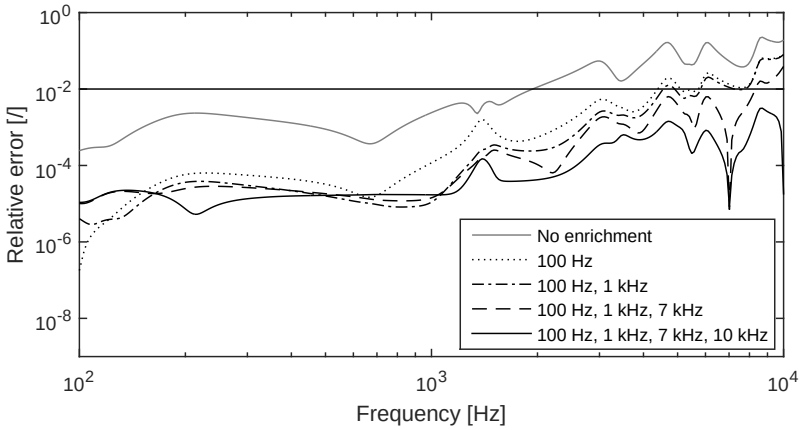

Figure 4: Reduction error for increasingly enriched reduction bases.

The construction of the reduction basis consists therefore of three main steps: solving the eigenvalue problem to obtain the modes up to 12 kHz, calculating 4 enrichment vectors, and orthogonalizing the resulting matrices to form $\mathbf{T}$. The time required for each step is detailed in Table 4, and adds up to 7.3 min. If the 9 s required for solving the reduced system and the 255 s required to obtain the matrices from ANSYS® (according to Table 3) are added to that, a total of 11.7 min are needed for a single objective function evaluation, which is 12 times faster than the 2.4 hours required when using the full system.

	Solving eigenvalue problem in ANSYS® and importing vectors into MATLAB®	Calculating enrichment vectors	Orthogonalizing matrices	Total
Time [s]	322	114	0.5	436.5 (7.3 min)

Table 4: Reduction basis construction computational times

3.2. Parametric model order reduction by adaptive basis construction

The approach described so far does not take into account the parametric dependency of the model. The reduced order basis could be re-computed for each combination of parameter values that needs to be evaluated during the optimization process, which has been shown to be 12 times more efficient than using

the full model. However, this approach would still be relatively time consuming compared to what can be achieved when using parametric Model Order Reduction (pMOR) techniques. Typically, pMOR methods consist in constructing a reduction basis "offline" (i.e. before the optimization) that is accurate throughout the parameter design domain, and the basis is then used throughout the optimization to reduce the system matrices, avoiding to solve the full system during the "online" phase [35].

The pMOR technique selected in this work consists in sampling the parameter design space and forming a global reduction basis by concatenating the basis vectors calculated at the different sample points. In the classical approach, the reduction basis should be formed by sampling the parametric space finely enough so that the obtained global basis introduces a reduction error below a required threshold throughout the full design domain. To ensure that, the error must be evaluated at a representative set of non sampled points, and new points must be added to the basis until the requirement is fulfilled [18]. This can become highly time consuming due to two factors: (1) the full model needs to be solved in order to calculate the error, which is computationally expensive, and (2) a large number of points must be added to the basis in order to represent the whole parameter space.

In this section, issues (1) and (2) are addressed. Firstly, a cheap pragmatic error indicator is presented. Secondly, a technique to reduce the number of points that need to be included in the reduction basis is introduced. The proposed approach exploits the fact that, during the optimization, a specific path within the design domain will be followed, and therefore only a small part of it will actually be evaluated. Consequently, there is no need to represent accurately the complete design domain, but only those areas that will actually be explored, as illustrated in Figure 5.

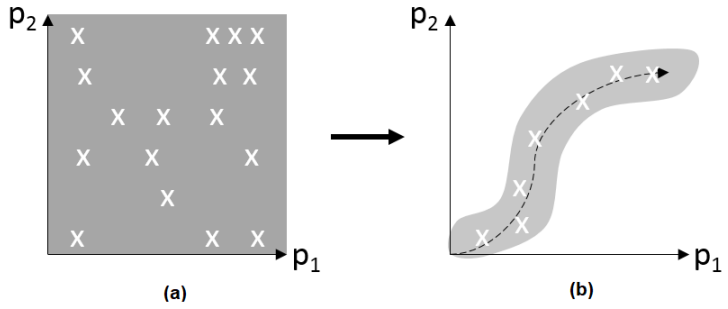

Figure 5: Traditional parameter sampling for reduction basis construction (a) and new adaptive approach (b) for an example with 2 parameters. The white crosses indicate points on the parameter space that are included in the reduction basis, and the dashed line represents the path followed during the optimization. The grey area indicates the parameter space where the reduction is accurate in each case.

3.2.1. Error indicator

Many *a posteriori* error indicators are based on the computation of the norm of residuals associated with the full model. The norm of the force residual can be computed relatively cheaply by inserting the reconstructed state vector into the full system equation of motion, i.e.

$$\Delta\mathbf{f} = \left(\mathbf{K} - \omega^2\mathbf{M}\right)\tilde{\mathbf{x}} - \mathbf{f}. \tag{16}$$

The force residual has been directly used as an error indicator in the literature [27, 21]. It measures how good of a solution to the system the reconstructed response is; however, we are concerned about how much the reconstructed response deviates from the full model response; therefore, we search for an estimate of the relative state vector error, as expressed in eq. (13). In the literature, most suggested approaches to approximating this error from the norm of the force residual are mainly concerned with reduction methods based on

Proper Orthogonal Decomposition (POD). POD consists in building the reduction basis from "snapshots" of the state vector at different parameter points, where the full system must be solved. The true error can directly be obtained at those points since the full system solution is available, and it is used in Ref. [24] to create a linear model between the norm of the force residual, $||\Delta\mathbf{f}||_2$, and the norm of the state vector residual, $||\Delta\mathbf{x}||_2 = ||\mathbf{x} - \tilde{\mathbf{x}}||_2$, which is then used to estimate the error at other points.

For modal-based reduction, the full system response is not calculated when building the reduction basis; therefore, this approach cannot be directly used. However, the idea of finding a relationship between the residual on the dynamic force balance and the state error may still be feasible. In practice, we observed that when the ROM is sufficiently accurate, there is close to a constant offset between the force residual and state vector error over the frequency range of interest, which is demonstrated in Figure 6. Therefore, as a pragmatic approximation, this offset could be calculated at one single frequency, f_0, and used to roughly approximate the state vector residual at the rest of the frequency range by multiplying it by the force residual,

$$k = \frac{||\Delta\mathbf{x}(f_0)||_2}{||\Delta\mathbf{f}(f_0)||_2}, \tag{17}$$

$$||\Delta\mathbf{x}(\omega)||_2 \approx k||\Delta\mathbf{f}(\omega)||_2. \tag{18}$$

Then, the relative error can be estimated as

$$\epsilon_{ind}(\omega) = \frac{k||\Delta\mathbf{f}(\omega)||_2}{||\tilde{\mathbf{x}}(\omega)||_2} \approx \epsilon(\omega) = \frac{||\Delta\mathbf{x}(\omega)||_2}{||\mathbf{x}(\omega)||_2}. \tag{19}$$

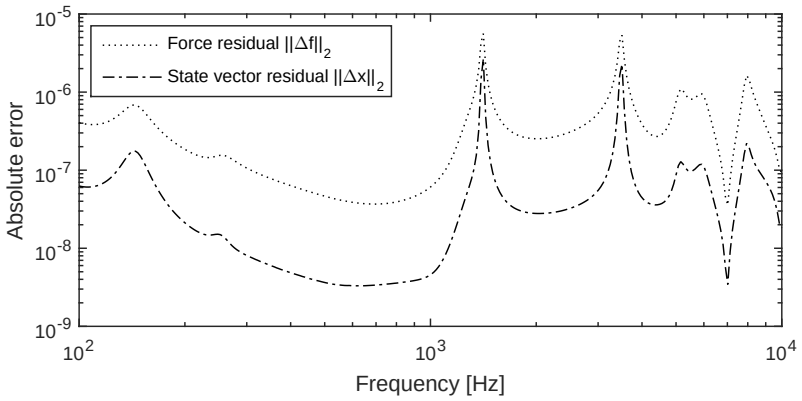

Figure 6: Comparison of the force residual and the state vector residual

The resulting estimated error, when f_0 is chosen at 5 kHz, is shown in Figure 7 in comparison to the true error. The curves are almost on top of each other in most of the frequency range, which shows that the indicator approximates well the sought error. If f_0 was chosen to be one of the frequencies at which the reduction basis enrichment vectors are calculated, $\mathbf{x}(f_0)$ would directly be available when calculating factor k for a point that is included in the reduction basis, which could reduce computational costs. However, the error can drop to very small values at those frequencies (as observed for example in Figure 4), which makes the ratio between the residuals at those frequencies not representative of the overall offset. Therefore, it is a better choice to select an f_0 far from the enrichment frequencies. Still, it is clear that the error indicator accuracy depends on the choice of f_0; moreover, the estimate deviates further from the true error when evaluating points that are far from the points included in the reduction basis, as in the case shown in Figure 8. There is therefore an uncertainty about the accuracy of the error indicator which must be taken into account. This is done by requiring a low value of the error indicator for a reduced model to be considered

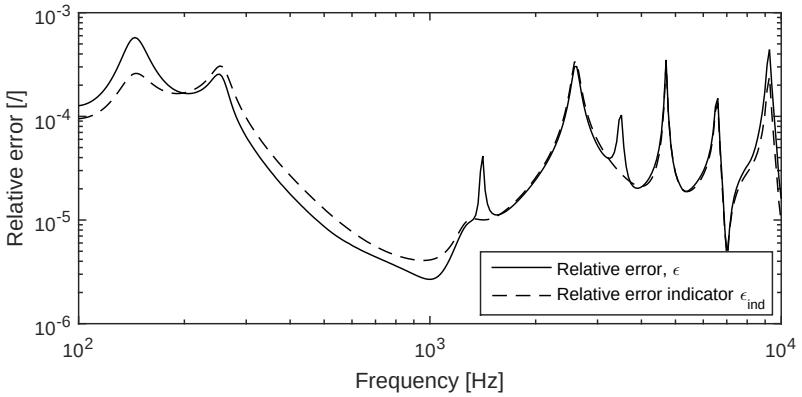

Figure 7: Comparison of the state vector true relative error and the error indicator

accurate enough; for example, allowing 0.5% as maximum value instead of the usual 1%. This solution proves effective in practice, as will be further discussed in section 4.

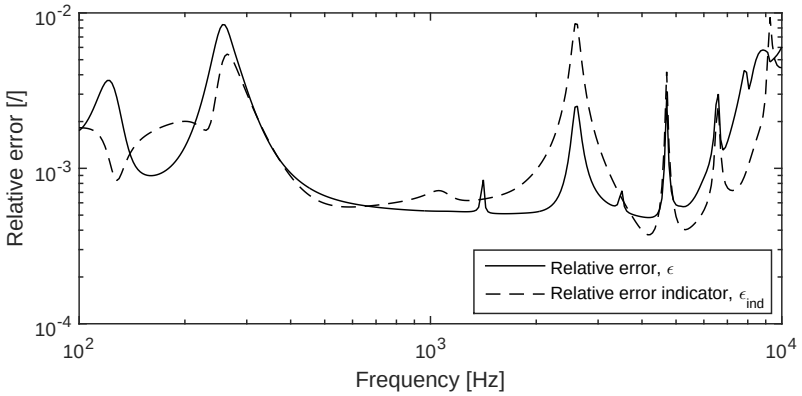

Figure 8: Comparison of the state vector true relative error and the error indicator at a point further from the points included in the basis

Even though the computation of the error indicator is cheap compared to solving the full system, the time required for the calculation is not negligible. The two most time-consuming steps are the calculation of $\mathbf{x}(f_0)$ for obtaining factor k and the calculation of the force residual, $\Delta\mathbf{f}(\omega)$, for a large number of frequencies. In the considered problem, the first step requires 29 s and the second step 74 s; this shows that checking the accuracy of the response still takes longer than the frequency response calculation itself, which took 9 s for the reduced system obtained in Section 3.1. The time consumption of each step in the calculations is further detailed in section 4.

3.2.2. Adaptive parametric model order reduction basis updating and optimization framework

A parameter space sampling method for the reduction basis construction that breaks the traditional offline-online approach is suggested here. The fact that only a specific path within the design domain is explored during the optimization is exploited to construct an efficient reduction basis that does not include information of the unexplored parts. Adaptive approaches for pMOR have been previously proposed by e.g. Zahr*et al.* [27]; however, they consist in solving a series of optimization problems in between which the

reduction basis is updated, while the algorithm suggested here embeds an *on-the-fly* basis updating routine into the optimization loop. The method works as follows:

- An initial reduction basis is calculated for the initial parameter set as shown in Section 3.1.
- During the optimization, a new parameter point is added to the global reduced order basis if the accuracy falls below a required level, which is checked by means of the suggested error indicator.

For the addition of a new point m to a reduction basis containing $m-1$ points, the global reduced order basis is obtained as follows. Maintaining the same philosophy as for the single-point reduction basis, the acoustic and structural modal matrices of each point included in the basis are concatenated separately, as

$$\boldsymbol{\Theta}_a = \left[\boldsymbol{\Psi}_a^1 \boldsymbol{\Psi}_a^2 ... \boldsymbol{\Psi}_a^{m-1} \boldsymbol{\Psi}_a^m\right] \tag{20}$$

$$\boldsymbol{\Theta}_s = \left[\boldsymbol{\Psi}_s^1 \boldsymbol{\Psi}_s^2 ... \boldsymbol{\Psi}_s^{m-1} \boldsymbol{\Psi}_s^m\right]. \tag{21}$$

The orthogonalization is then done on these global matrices, which reduces their size significantly in practice, since many modal vectors calculated for different parameter values are (close to) linearly dependent and therefore eliminated. The same approach is taken to obtain the global enrichment vector matrices,

$$\mathbf{Y}_a = \left[\mathbf{X}_a^1 \mathbf{X}_a^2 ... \mathbf{X}_a^{m-1} \mathbf{X}_a^m\right] \tag{22}$$

$$\mathbf{Y}_s = \left[\mathbf{X}_s^1 \mathbf{X}_s^2 ... \mathbf{X}_s^{m-1} \mathbf{X}_s^m\right], \tag{23}$$

and the global reduction basis is then formed by concatenating the orthagonalized global modal and enrichment matrices,

$$\mathbf{T} = \begin{bmatrix} \left[\hat{\boldsymbol{\Theta}}_s \hat{\mathbf{Y}}_s\right] & [\mathbf{0}] \\ [\mathbf{0}] & \left[\hat{\boldsymbol{\Theta}}_a \hat{\mathbf{Y}}_a\right] \end{bmatrix}. \tag{24}$$

Algorithm 1 describes the procedure for one objective function evaluation using the suggested adaptive reduction scheme. Firstly, the system is reduced with the current reduction basis and the response is calculated. The accuracy of the solution is checked by calculating the error indicator as in eq. (19) and detecting if its value is below a specified threshold, τ. If the error indicator is above the threshold, the current point is added to the reduction basis, which means that the modal vectors are obtained from ANSYS® , the enrichment components are calculated, and both sets are added to the global transformation matrix as specified in eqs. (20)-(24). The non-orthogonalized modal and enrichment matrices, Y_a, Y_s, Θ_a and Θ_s, are stored so that the orthogonalization is always done with respect to the mass matrices at the last added parameter point. Since the memory required for storing the matrices and the computational cost of orthogonalizing them grows with their size, a limitation (M) to the number of points that the reduction basis can contain is set. If the basis already contains M points when a new one is to be added, the first point in the basis is discarded, since it is assumed to be the furthest and therefore least relevant to the current point.

Algorithm 1: Objective function evaluation with apMOR

$[g, \mathbf{T}] = \mathit{ReducedObjectiveFunction}(\boldsymbol{\mu}, \mathbf{T}, \tau, M, \boldsymbol{\omega})$;

Input : Design parameters $\boldsymbol{\mu}$, current reduced order basis $\mathbf{T}$, reduction tolerance τ, maximum number of sample points in basis M, frequency lines $\boldsymbol{\omega}$

Output: Goal function g, updated reduced order basis $\mathbf{T}$

Get model matrices $\mathbf{K}, \mathbf{M}$ from ANSYS for design parameters $\boldsymbol{\mu}$;

Perform model reduction: $\mathbf{K}_r = \mathbf{T}^T\mathbf{K}\mathbf{T}$, $\mathbf{M}_r = \mathbf{T}^T\mathbf{M}\mathbf{T}$;

Solve the reduced system $\left(\mathbf{K}_r - \omega^2\mathbf{M}_r\right)\mathbf{x}_r = \mathbf{f}_r$ and obtain the reconstructed vector as $\tilde{\mathbf{x}} = \mathbf{T}\mathbf{x}_r$ for all frequency lines in $\boldsymbol{\omega}$;

Evaluate error indicator ϵ_{ind} using Eqs. (17)-(19);

if $\epsilon_{ind} \geq \tau$ **then**

  if *M sample points in* $\mathbf{T}$ **then**

    Remove first point from global bases: $\boldsymbol{\Theta}_a := [\boldsymbol{\Psi}_a^2 \dots \boldsymbol{\Psi}_a^M]$, $\boldsymbol{\Theta}_s := [\boldsymbol{\Psi}_s^2 \dots \boldsymbol{\Psi}_s^M]$, $\mathbf{Y}_a := [\mathbf{X}_a^2 \dots \mathbf{X}_a^M]$, $\mathbf{Y}_s := [\mathbf{X}_s^2 \dots \mathbf{X}_s^M]$;

  end

  Calculate enriched modal basis $\boldsymbol{\Psi}_a^m, \boldsymbol{\Psi}_s^m, \mathbf{X}_a^m, \mathbf{X}_s^m$ for parameters $\boldsymbol{\mu}$;

  Set up new global bases, orthogonalize them and update $\mathbf{T}$ according to Eqs. (20)-(24);

  Perform model reduction: $\mathbf{K}_r = \mathbf{T}^T\mathbf{K}\mathbf{T}$, $\mathbf{M}_r = \mathbf{T}^T\mathbf{M}\mathbf{T}$;

  Solve the reduced system $\left(\mathbf{K}_r - \omega^2\mathbf{M}_r\right)\mathbf{x}_r = \mathbf{f}_r$ and obtain the reconstructed vector as $\tilde{\mathbf{x}} = \mathbf{T}\mathbf{x}_r$ for all frequency lines in $\boldsymbol{\omega}$;

end

Evaluate objective function g from Eq. (2);

The proposed adaptive parametric Model Order Reduction (apMOR) technique can be used in combination with any existing optimization algorithm. In this work, the gradient-based constrained optimization algorithm implemented in the MATLAB Optimization Toolbox function *fmincon* [30] is used, with the gradient being calculated by Finite Differences (FD). At each iteration of the optimization routine, Algorithm 1 is called several times since several objective function evaluations are required for gradient calculation and decision of the next parameter point.

4. Application results

The results obtained for the optimization problem introduced in Section 2 using the suggested apMOR method are discussed here. The thickness and E-modulus of both the tube and the suspension are optimized within the given design space in order to minimize the total velocity at the microphone position over a frequency range between 100 Hz and 10 kHz, when the receiver excites the system with the signals shown in Figure 2.

4.1. Considerations on the optimization setup

Given that the gradient of the objective function is calculated by FD, at least 5 objective function evaluations are needed at each iteration of the optimization algorithm. Since the accuracy of the reduced system is checked at each objective function evaluation, it is crucial to make the calculation of the error indicator as efficient as possible. As mentioned in Section 3.2.1, updating factor k is relatively time consuming since it requires solving the full system at one frequency. Based on the assumption that the value of k only experiences large variations when the reduction basis is modified or when the parameter values vary significantly, the approach taken here to speed up the process consists in updating k only when a new point is added to the basis and at the start of each *fmincon* iteration. For the rest of objective function evaluations, ϵ_{est} is

calculated using the last updated k value and only the force residual needs to be computed, which saves 29 seconds per evaluation.

The maximum number of points allowed in the reduction basis, M, and the threshold on the error indicator for which the reduction is considered accurate, τ, must be specified beforehand. The first parameter is set here to 5, which has been selected as a trade-off between accuracy and the computational cost required for orthogonalization of the basis. Regarding parameter τ, a value of $5 \cdot 10^{-3}$ (0.5%) is chosen, which is more restrictive than the 1% threshold that would be recommended if the true error was being evaluated instead of an error indicator, and also leaves a small margin with respect to the maximum error at the initial point, shown in Figure 4, which was $3 \cdot 10^{-3}$. In general, the error decreases when increasing the number of points included in the reduction basis; therefore, it should always be below this threshold when a new point is added.

4.2. Optimization results

The optimization reached convergence after 12 iterations of the *fmincon* algorithm, which required 63 objective function evaluations. During the process, 7 points of the parameter space were added to the reduction basis besides the initial point, which adds up to 8 points in total, and therefore the 3 first points were removed from it during the process to fulfill the selected 5 point limitation. In total, the optimization process took 7 hours and 40 minutes; if the full system had been used, 153 hours would have been needed for 63 function evaluations, given that each one takes 2.4 hours as shown in Table 3. Therefore, the suggested method speeds up the optimization by a factor of 20.

The time required for a function evaluation with the reduced system varies according to the steps needed and size of the reduced system at each point. The times required for each step are detailed in Table 5, where the minimum total time is given for an evaluation where factor k is not calculated and no new point is added to the basis, and the total maximum is for an evaluation where a new point is added (and therefore the response and error indicator are calculated twice). For the upper bound, the function evaluation is 9 times faster than for the full system, which shows that even in the worst case scenario a significant speed-up is achieved.

	Building matrices in ANSYS® and importing into MATLAB®	Reducing system and solving @ 300 freq. lines (min. - max.)	Calculating k factor [eq.(17)]	Evaluating $\Delta\mathbf{f}$ [eq.(16)] and ϵ_{est} [eq.(19)]	Adding point to basis (Table 4)	Total (min. - avg. - max.)
Time [s]	255	9 - 44	29	73	436.5	337 - 438 - 983 (5.6 - 7.3 - 16.4 mins)

Table 5: Computational time spent at different objective function evaluation steps and total minimum, average and maximum time per evaluation, calculated depending on the required steps at each evaluation according to the Algorithm 1.

The total reduction on the objective function value was of 3.4 dB, which was reached for the parameter values in Table 6. The suspension parameters experienced the largest changes with respect to the initial point, while the tube parameters varied very slightly. The initial and final curves of the total velocity at the microphone position are shown in Figure 9, where it can be observed that the first peak has been shifted down in frequency as a result of the decrease on the suspension Young's modulus. The peak at 1330 Hz (originated by a peak on the excitation signals) cannot be shifted but is attenuated due to the lower mode overlap resulting from the shift of the first peak. The dotted curve in Figure 9 shows the velocity curve calculated with frequency dependent losses for the optimized parameters in order to verify that the frequency independent BLI approximation used in the optimization yields realistic results. The differences

with respect to the solid curve are small and occur mainly at very low velocity levels, which confirms that the introduced approximation yields meaningful results.

	$\boldsymbol{\mu}_{out}$
Tube E modulus [Pa]	$1.8 \cdot 10^8$
Tube thickness [mm]	0.973
Suspension E modulus [Pa]	$1 \cdot 10^6$
Suspension thickness [mm]	0.175

Table 6: Final parameter values

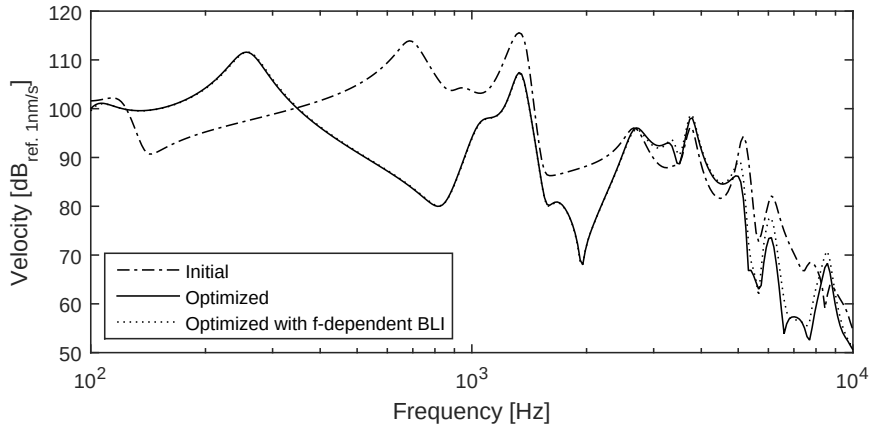

Figure 9: Total velocity at the microphone position at the initial and final points of the optimization

The evolution of the error indicator maximum value with respect to the objective function evaluations is shown in Figure 10, where the dotted vertical lines indicate the start of a new iteration. The evaluations where the error is above the required threshold τ (indicated by the solid horizontal line) present two values, the circled asterisk being the error before adding the current point to the reduction basis, and the simple asterisk indicating the error after the update. At the function evaluation number 23, the fifth basis update takes place, which means that the basis is now formed by 6 points in total. Therefore, the initial point is removed from it, and the value marked by the simple asterisk is the error after addition of the new point and removal of the first point, which is kept below the required threshold. The same procedure is followed at the function evaluations 27 and 28, keeping the total number of points in the basis at 5. The error estimate at the final point is shown in Figure 4 in comparison with the true error, where it can be seen that the shapes are slightly different, but the values oscillate within the same range.

The objective function and parameter k values at each iteration are shown in Figures 12(a) and 12(b). The objective function value experiences its largest change at iteration 1, and it decreases slowly thereafter. Therefore, the largest parameter changes occur at the beginning of the optimization, which explains that the first basis updates take place during iterations 0 and 1, and, after a few updates in iterations 4 and 5, the reduction basis remains unchanged at the second half of the optimization, as shown in Figure 10. The k value, which is only updated when a point is added or removed from the basis and at the start of each iteration, presents the largest variations within the first 6 iterations, which also correlates with the fact that the reduction basis is being updated in those. Even though it is recalculated at each iteration thereafter, the variations are very small from iteration 7, confirming that it does not change significantly when the parameter variations are small. The fact that no basis updates are needed after iteration 5 makes

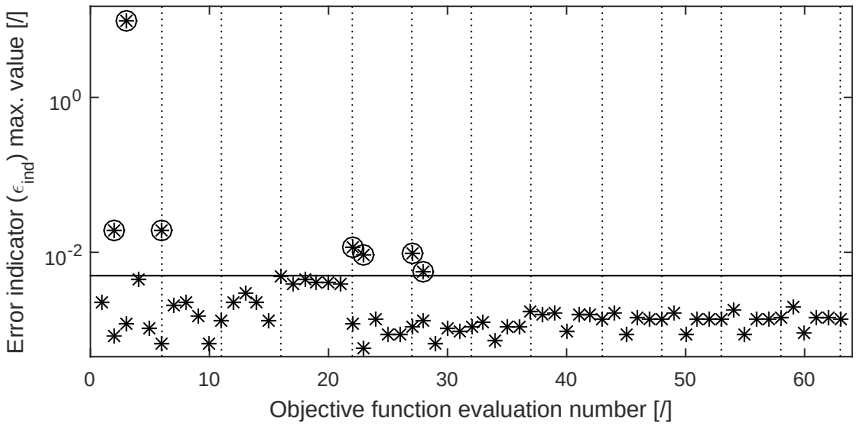

Figure 10: Evolution of the maximum value of the error indicator vs. objective function evaluations. Simple asterisks: error estimate at the end of the objective function evaluation. Circled asterisks: error estimate before reduction basis update at parameter points that are added to the basis.

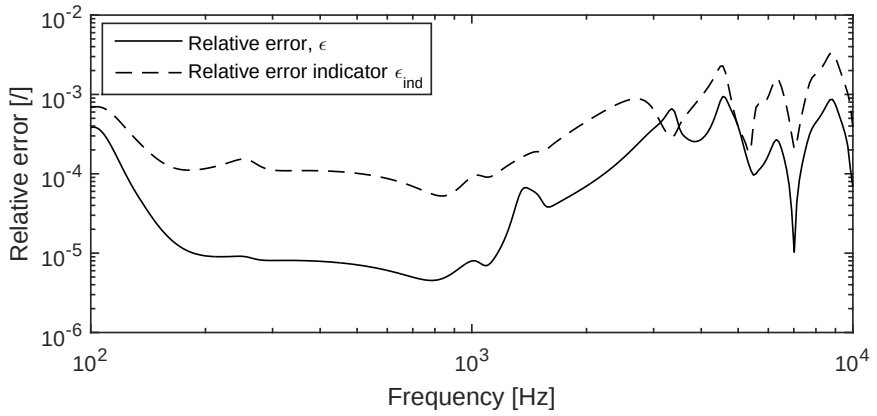

Figure 11: Comparison of the state vector true relative error and the error indicator at the final point

the final part of the optimization very fast, corroborating that the suggested method is specially powerful for gradient-based optimization problems, where the final steps require many function evaluations around the last point in order to detect convergence.

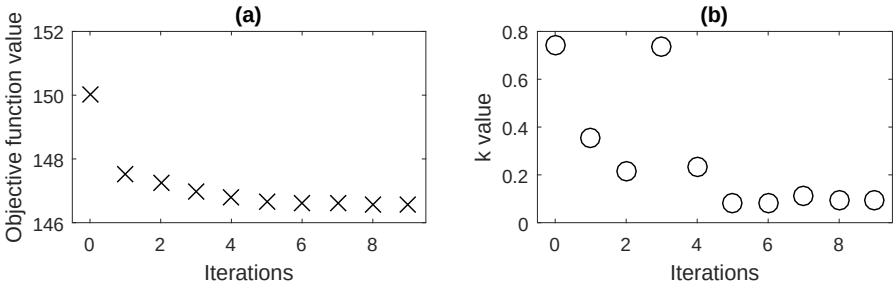

Figure 12: (a) Evolution of the objective function. (b) Parameter k during the optimization.

4.3. Discussion

Even though frequency dependency is not considered in the suggested modal-based reduction approach, visco-thermal losses have been considered by applying a frequency independent approximation that has been shown not to introduce a significant error to the optimization results in the studied case. However, it would be interesting to include other frequency dependent properties that are relevant in the field of hearing aids as well as in others, such as material data or transducer models, for which the suggested method could be extended by considering frequency as an extra parameter, as for example in Refs. [36, 37]. Moreover, modelling the air that surrounds the hearing aid would also be desired in order to optimize for the acoustic pressure outside; in that case, calculating the modes can become computationally time consuming since it is challenging to calculate only those modal vectors that are necessary for model reduction in an infinite acoustic domain [38]. Therefore, other techniques such as rational interpolation methods [4] could be a better choice for obtaining a reliable reduction basis, as done in Ref. [39].

The error indicator has been developed as a trade-off between accuracy and computational cost. The accuracy could have been improved by calculating the k factor at several frequencies and taking an average, or by updating it at each objective function evaluation; however, the extra computational time that this would require is not worthwhile in practice, since it has been shown that the true error at the final point is well below the required level, and therefore the used approximation fulfills the purpose for which the error indicator was intended.

Regarding the suggested adaptive parameter sampling algorithm, it is worth noting that the traditional offline-online approach might be more efficient for other applications of parametrized models such as system control, where the speed of the reduced system evaluations during the online phase is crucial, and justifies having a long offline phase where an accurate global basis is obtained. However, in the context of optimization and related applications such as model updating and inverse problems, the reduction basis will rarely be re-used, and the most important factor is the total time that the optimization takes, including reduction basis construction.

To confirm that the suggested approach is more efficient for the discussed case, an approximation of the time that would be required with the offline-online approach can be done from the previous work by the authors presented in Ref. [15], where a simpler version of the hearing aid model presented here was optimized for 2 parameters. In order to build the global reduction basis offline, 4 parameter points were needed, corresponding to the combination of all the extreme values. From that, it can be extrapolated that at least 16 points would be needed when considering 4 parameters as in the current work, for which the reduction

basis would take 2 hours to be built considering the times given in Table 4. According to Table 5, reducing the system and solving it takes 44 s for a reduction basis with 5 points; from that, we can approximate that it would take about 140 s for a basis with 16 points. Adding the time spent on interfacing with ANSYS® , the online phase would then take about 7 hours assuming that 63 objective function evaluations would be needed as well. The complete process would take 9 hours, which is longer than the time required by the suggested apMOR technique (7.6 hours). Moreover, the time that should be spent in checking the reduction error during the offline phase has not been included in this approximation, which would make the time difference significantly larger in reality.

5. Conclusions

An adaptive algorithm for parametric Model Order Reduction (pMOR) basis construction in optimization problems that updates the reduction basis automatically along the optimization loop avoiding previous parameter space sampling has been presented. The method relies on a newly developed residual-based error indicator to ensure a selected accuracy of the reduction basis at all evaluated points. An enriched modal-based reduction method has been developed, which overcomes the orthogonalization issues that arise from the non-symmetric nature of the vibroacoustic system matrices when the pressure-displacement formulation is used. The performance is demonstrated for a classical optimization problem from the hearing aid field where the feedback between the loudspeaker and the microphone is to be minimized within a wide frequency range (100 Hz to 10 kHz), where the objective function evaluation requires fine resolution frequency response calculation. The suggested method is shown to be efficient in such context, since the average objective function evaluation time is 20 times shorter than if using the full model. Further validation of the proposed methodology by means of experimental measurements of the optimized solution is left as future work.

6. Acknowledgments

The authors would like to thank the Innovation Fond Denmark and the Oticon Foundation for their financial support.

References

[1] M. B. Sondergaard, C. B. W. Pedersen, Applied topology optimization of vibro-acoustic hearing instrument models, Journal of Sound and Vibration 333 (3) (2014) 683–692. doi:10.1016/j.jsv.2013.09.029.

[2] B. Besselink, U. Tabak, A. Lutowska, N. van de Wouw, H. Nijmeijer, D. Rixen, M. Hochstenbach, W. Schilders, A comparison of model reduction techniques from structural dynamics, numerical mathematics and systems and control, Journal of Sound and Vibration 332 (19) (2013) 4403 – 4422. doi:http://dx.doi.org/10.1016/j.jsv.2013.03.025. URL http://www.sciencedirect.com/science/article/pii/S0022460X1300285X

[3] P. Koutsovasilis, M. Beitelschmidt, Comparison of model reduction techniques for large mechanical systems, Multibody System Dynamics 20 (2) (2008) 111–128. doi:10.1007/s11044-008-9116-4.

[4] P. Benner, S. Gugercin, K. Willcox, A survey of projection-based model reduction methods for parametric dynamical systems, Siam Review 57 (4) (2015) 483–531. doi:10.1137/130932715.

[5] R. R. Craig, M. C. C. Bampton, Coupling of substructures for dynamic analyses, AIAA Journal 6 (7) (1968) 1313–1319.

[6] R. R. Craig, Coupling of substructures for dynamic analyses: an overview, Collection of Technical Papers - AIAA/ASME/ASCE/AHS/ASC Structures, Structural Dynamics and Materials Conference 5 (2000) 3–14.

[7] J. Wolf, Modal synthesis for combined structural-acoustic systems, AIAA Journal 15 (5) (1977) 743–745. doi:10.2514/3.60685.

[8] P. Davidsson, G. Sandberg, A reduction method for structure-acoustic and poroelastic-acoustic problems using interface-dependent lanczos vectors, Computer Methods in Applied Mechanics and Engineering 195 (17-18) (2006) 1933–1945. doi:10.1016/j.cma.2005.02.024.

[9] Z. Ma, I. Hagiwara, Improved mode-superposition technique for modal frequency-response analysis of coupled acoustic-structural systems, AIAA Journal 29 (10) (1991) 1720–1726. doi:10.2514/3.10795.

[10] M. Stammberger, H. Voss, Automated multi-level substructuring for a fluid-solid vibration problem, Numerical Mathematics and Advanced Applications (2008) 563–570.

[11] M. Maess, L. Gaul, Substructuring and model reduction of pipe components interacting with acoustic fluids, Mechanical Systems and Signal Processing 20 (1) (2006) 45–64. doi:10.1016/j.ymssp.2005.02.008.

[12] E. Creixell-Mediante, J. S. Jensen, J. Brunskog, M. Larsen, A multi-model reduction technique for optimization of coupled structural-acoustic problems, Proceedings of Inter-noise 2016 (2016) 7601–7612.

[13] S. Donders, B. Pluymers, P. Ragnarsson, R. Hadjit, W. Desmet, The wave-based substructuring approach for the efficient description of interface dynamics in substructuring, Journal of Sound and Vibration 329 (8) (2010) 1062–1080. doi:10.1016/j.jsv.2009.10.022.

[14] J. Herrmann, M. Maess, L. Gaul, Substructuring including interface reduction for the efficient vibro-acoustic simulation of fluid-filled piping systems, Mechanical Systems and Signal Processing 24 (1) (2010) 153–163. doi:10.1016/j.ymssp.2009.05.003.

[15] E. Creixell-Mediante, J. S. Jensen, J. Brunskog, M. Larsen, Model reduction for optimization of structural-acoustic coupling problems, Proceedings of Isma 2016.

[16] C. Pal, I. Hagiwara, Dynamic analysis of a coupled structural-acoustic problem - simultaneous multimodal reduction of vehicle interior noise level by combined optimization, Finite Elements in Analysis and Design 14 (2-3) (1993) 225–234. doi:10.1016/0168-874x(93)90022-i.

[17] L. Hermans, M. Brughmans, Enabling vibro-acoustic optimization in a superelement environment: A case study, Proceedings of the International Modal Analysis Conference and Exhibit 2 (2000) 1146–1152.

[18] E. Balmès, Parametric families of reduced finite element models. theory and applications, Mechanical Systems and Signal Processing 8 (8) (1994) 381–394. doi:10.1006/mssp.1996.0027.

[19] M. Drohmann, K. Carlberg, The romes method for statistical modeling of reduced-order-model error, Siam/asa Journal on Uncertainty Quantification 3 (1) (2015) 116–45, 116–145. doi:10.1137/140969841.

[20] A. Quarteroni, G. Rozza, A. Manzoni, Certified reduced basis approximation for parametrized partial differential equations and applications, Journal of Mathematics in Industry 1 (1) (2011) 1–49. doi:10.1186/2190-5983-1-3.

[21] U. Hetmaniuk, R. Tezaur, C. Farhat, An adaptive scheme for a class of interpolatory model reduction methods for frequency response problems, International Journal for Numerical Methods in Engineering 93 (10) (2013) 1109–1124. doi:10.1002/nme.4436.

[22] G. Rozza, An introduction to reduced basis method for parametrized pdes, Series on Advances in Mathematics for Applied Sciences 82 (2010) 508–519.

[23] A. Manzoni, A. Quarteroni, G. Rozza, Computational reduction for parametrized pdes: Strategies and applications, Milan Journal of Mathematics 80 (2) (2012) 283–309. doi:10.1007/s00032-012-0182-y.

[24] A. Paul-Dubois-Taine, D. Amsallem, An adaptive and efficient greedy procedure for the optimal training of parametric reduced-order models, International Journal for Numerical Methods in Engineering 102 (5) (2015) 1262–1292. doi:10.1002/nme.4759.

[25] T. Bui-Thanh, K. Willcox, O. Ghattas, Model reduction for large-scale systems with high-dimensional parametric input space, Siam Journal on Scientific Computing 30 (6) (2008) 3270–3288. doi:10.1137/070694855.

[26] Y. Yue, K. Meerbergen, Accelerating optimization of parametric linear systems by model order reduction, Siam Journal on Optimization 23 (2) (2013) 1344–1370. doi:10.1137/120869171.

[27] M. J. Zahr, C. Farhat, Progressive construction of a parametric reduced-order model for pde-constrained optimization, International Journal for Numerical Methods in Engineering 102 (5) (2015) 1111–1135. doi:10.1002/nme.4770.

[28] C. Gogu, Improving the efficiency of large scale topology optimization through on-the-fly reduced order model construction, International Journal for Numerical Methods in Engineering 101 (4) (2015) 281–304. doi:10.1002/nme.4797.

[29] R. Bossart, N. Joly, M. Bruneau, Hybrid numerical and analytical solutions for acoustic boundary problems in thermo-viscous fluids, Journal of Sound and Vibration 263 (1) (2003) 69–84.

[30] MATLAB optimization toolbox user's guide R2015b, MathWorks, Natick, MA, 2015.

[31] R. H. Byrd, M. E. Hribar, J. Nocedal, An interior point algorithm for large-scale nonlinear programming, Siam Journal on Optimization 9 (4) (1999) 877–900. doi:10.1137/S1052623497325107.

[32] ANSYS, Inc., ANSYS Academic Research, Release 17.1, Help System, Theory Reference.

[33] G. Golub, C. van Loan, Matrix computations, The Johns Hopkins University Press, 1996.

[34] D. J. Rixen, Generalized mode acceleration methods and modal truncation augmentation, 19th AIAA Applied Aerodynamics Conference.

[35] P. Benner, S. Gugercin, K. Willcox, A survey of model reduction methods for parametric systems, Max Planck Institute Magdeburg Preprint MPIMD/13-14, available from *http://www.mpi-magdeburg.mpg.de/preprints/*.

[36] Z. S. Chen, G. Hofstetter, H. A. Mang, A 3d boundary element method for determination of acoustic eigenfrequencies considering admittance boundary conditions, Journal of Computational Acoustics 1 (4) (1993) 455–468. doi:10.1142/S0218396X93000238.

[37] H. Peters, N. Kessissoglou, S. Marburg, Modal decomposition of exterior acoustic-structure interaction problems with model order reduction, Journal of the Acoustical Society of America 135 (5) (2014) 2706–2717. doi:10.1121/1.4869086.

[38] L. Moheit, S. Marburg, Infinite elements and their influence on normal and radiation modes in exterior acoustics, Journal of Computational Acoustics 25 (04) (2017) 1650020. doi:10.1142/S0218396X1650020X.

[39] A. van de Walle, Y. Shiozawa, H. Matsuda, W. Desmet, Model order reduction for the transient vibro-acoustic simulation of acoustic guitars, Proceedings of Isma2016 International Conference on Noise and Vibration Engineering and Usd2016 International Conference on Uncertainty in Structural Dynamics (2016) 4007–4017.